JIRBDAI Journal of Institutional Research, Big Data Analytics and Innovation

DEVELOPMENT OF A DEEP LEARNING APPROACH FOR OVARIAN CYSTS DETECTION AND CLASSIFICATION USING ADARESU-NET

Toyin Okebule, Ajewole Femi
Department of Computer Science, Faculty of Computing, Federal University of Technology and Environmental Sciences Iyin-Ekiti, Nigeria
slimtoyin2003@gmail.com, *ogunsfemi366@gmail.com*

ABSTRACT: Ovarian cysts are common gynaecological conditions that require accurate and timely detection to guide clinical decisions and prevent complications. Early and accurate detection of ovarian cysts is critical for timely clinical intervention and effective patient management. Conventional diagnostic techniques, such as ultrasound imaging, often depend heavily on the expertise of clinicians, making automated detection methods highly desirable. The application of an adaptive residual U-Net (AdaResUNet) architecture for the segmentation and detection of ovarian cysts in ultrasound images was employed for this study. AdaResUNet combines the strengths of U-Net for semantic segmentation with residual learning and adaptive feature recalibration to enhance model performance on complex medical imaging tasks. A balanced dataset of 700 cyst images (400 for training and 300 for testing) were sourced from OASIS and OC400 dataset. The model recorded recall of 98.5%, precision of 98.4%, F1 Score of 98.8%, and accuracy of 99.9%, showing strong performance. The network incorporates attention mechanisms and deep residual blocks to improve feature propagation, gradient flow, and localization accuracy. The results suggest that AdaResUNet can serve as a reliable tool to assist clinicians in the early diagnosis and management of ovarian cysts, potentially improving patient outcomes.

KEYWORDS: Ovarian Cysts, Deep Learning Model, Adaresunet Model, Guided Bilateral Filter, Confusion Matrix.

I. INTRODUCTION

Ovarian cysts pose significant health risks including torsion, infertility, and cancer, necessitating rapid and accurate diagnosis. Ovarian cysts are fluid-filled cases that form on or within the ovaries and are common among women of reproductive age. While many ovarian cysts are benign and asymptomatic, others may lead to complications such as rupture, torsion, or malignancy if left undiagnosed or untreated. Accurate and early detection of ovarian cysts is therefore essential for appropriate clinical management, reducing the risk of adverse outcomes and improving patient prognosis [1]. Ultrasound imaging, particularly transvaginal ultrasonography, remains the primary diagnostic tool for evaluating ovarian cysts due to its non-invasive nature, accessibility, and cost-effectiveness. However, manual interpretation of ultrasound images is highly operator-dependent and may be influenced by subjective judgment, leading to diagnostic variability and potential oversight of subtle cystic structures [1]. In recent years, infertility has emerged as a significant concern among individuals of reproductive age. A study conducted by the World Health Organization on 8500 infertile couples revealed that male infertility accounted for 8% of cases, while female infertility and a combination of both contributed to 37% and 35% respectively. Additionally, 5% of the couples experienced unexplained infertility, and 15% were able to conceive during the study [2]. Various factors were identified as contributors to female infertility, including ovulatory dysfunction (25%), unexplained infertility (20%), endometriosis (15%), fallopian tube issues (22%), pelvic disorders (12%), and hyperpro-lactinemia (7%). Notably, ovarian cysts were found to be a common cause of female infertility, affecting a majority of infertile women [3].An advances in artificial intelligence (AI) and deep learning have shown significant promise in medical imaging analysis. Convolutional neural

Volume 2, Issue 2, 2026
https://doi.org/10.5281/zenodo.20678563

networks (CNNs), in particular, have demonstrated remarkable success in image classification, object detection, and segmentation tasks. Among these, U-Net and its variants have been widely adopted for biomedical image segmentation due to their ability to learn from limited datasets and produce accurate pixel-level predictions [4]. To further enhance performance, especially in challenging medical imaging scenarios, adaptive models such as AdaResUNet have been proposed to improve the network's capacity and learn complex spatial features and enhancing its robustness to variations in image quality and anatomical structures. Applying such advanced architectures to ovarian cyst detection holds great potential for improving diagnostic consistency and accuracy [5]. Previous researchers have employed different artificial intelligence techniques to segment the cysts; however, achieving accuracy and reducing processing time still present obstacles. To overcome these challenges, this study proposes an adaptive deep learning-based segmentation technique using a database of ovarian ultrasound cyst images.

II. REVIEW OF RELATED WORK

To gain an in-depth knowledge on this study, thorough literature review was carried out based on different methods and performances achieved in existing works:

Giourga et al. IN [6] investigated the application of convolutional neural networks (CNNs) for classifying ovarian masses from ultrasound imaging. Their dataset comprised 3,510 ultrasound scans collected from 585 women, annotated and validated by radiologists. They evaluated several pre-trained architectures, including VGG16, ResNet50, and InceptionNet, both individually and as an ensemble. The ensemble framework achieved the strongest diagnostic performance, reaching a sensitivity of 96.5% and specificity of 88.1% when applying a 0.2 probability threshold. These results highlight the clinical promise of CNN-based ensembles in supporting ovarian mass diagnosis, outperforming single models in robustness and generalization. However, the reliance on a single-center dataset without external validation limits the model's applicability across diverse clinical environments, and further studies are necessary to evaluate its performance in real-world multicenter settings. Xia et al. in [7] conducted a comparative analysis of deep learning algorithms against the O-RADS scoring system and expert radiologist reviews for predicting ovarian tumor malignancy from ultrasound images. Their study demonstrated that deep learning models preserved specificity close to 80% at clinically relevant sensitivity thresholds. Nevertheless, their overall diagnostic accuracy consistently remained below 90%. Detailed confusion matrix analysis revealed particular difficulties in distinguishing borderline tumors, which often overlapped with both benign and malignant categories. This highlighted the inherent complexity of ovarian tumor classification and the limitations of current algorithms when applied to intermediate-risk lesions. However, this study only utilized selected static images rather than full ultrasound video sequences and lacked prospective clinical testing, reducing its direct clinical translatability.

Another study in [8] developed a deep learning-based segmentation framework for identifying ovarian cancer lesions on CT scans. The system was benchmarked against the "no-new-Net" architecture and achieved a mean Dice similarity coefficient of 71 ± 20 for pelvic/ovarian lesions and 61 ± 24 for omental lesions. Remarkably, the model's performance was comparable to that of a trainee radiologist, underlining the potential of AI-assisted lesion delineation in oncology imaging. This approach has important implications for surgical planning and therapy monitoring by providing consistent lesion quantification. However, the limited sample size and imbalanced representation of lesion categories restrict the model's general applicability, and larger multicenter studies are needed to ensure robust generalization. In a study, Gao et al. [9] constructed a deep convolutional neural network for ovarian cancer detection using a very large dataset of 34,488 pelvic ultrasound images sourced from multiple centers across China. The model achieved strong generalizability, with AUC values of 0.911 on the internal dataset, 0.870 on the first external dataset, and 0.831 on a second independent validation set. Despite these promising results, analysis of confusion matrices revealed a persistent challenge in accurately classifying borderline tumors, which were frequently misclassified as either benign or malignant. The multicenter design of the dataset strengthens the study's external relevance, offering evidence for AI integration into ovarian cancer screening workflows. However, further studies are required, particularly prospective clinical trials, to

Volume 2, Issue 2, 2026
https://doi.org/10.5281/zenodo.

assess the model's real-time clinical utility and long-term diagnostic reliability. Another author in [10] introduced a novel pipeline known as OvaMTA, which integrates segmentation and classification modules for automated ovarian mass diagnosis from ultrasound. The system was trained on 6,938 images and externally validated on 1,584 cases from 21 hospitals, making it one of the more broadly validated models in this domain. OvaMTA-Seg, the segmentation module, achieved Dice scores of 0.887 on internal and 0.819 on external datasets, while OvaMTA-Diagnosis, the classification module, attained an AUC of 0.941 across multiple cohorts. These results underscore the clinical promise of combining segmentation with diagnostic classification for reliable, large-scale deployment. However, despite its robust design, real-time deployment in routine clinical practice has not yet been realized, and additional work is needed to address workflow integration and physician adoption.

Chen et al. in [11] developed a deep learning framework based on contrast-enhanced computed tomography (CECT) to differentiate between benign and malignant ovarian tumors. Their model was trained and validated on 1,329 patients, with additional prospective validation in 472 cases. They reported a sensitivity of 89% and specificity of 81%, achieving an overall AUC of 0.92. Importantly, their study demonstrated that deep learning outperformed traditional radiomics approaches and even matched the performance of senior radiologists in several test scenarios. This reinforces the clinical potential of CT-based deep learning for preoperative ovarian cancer risk stratification. However, the study was limited by its dependence on a single imaging modality, more so, the lack of integration with ultrasound or clinical biomarkers may restrict the model's real-world diagnostic scope. Another study in [12] proposed a deep learning-based radiomics model for ovarian tumor classification using multi-parametric MRI. Their dataset consisted of 1,041 women, and the model was benchmarked against expert radiologists. The deep learning model achieved an AUC of 0.94 compared to 0.91 for radiologists, highlighting its potential as a decision-support tool. Feature analysis revealed that the network captured textural and morphological patterns not easily discernible by the human eye. Despite these promising findings, the study relied heavily on high-quality MRI scans that may not always be feasible in resource-limited healthcare systems. Additionally, the black-box nature of the model limits interpretability, which is crucial for clinical adoption. Qian et al. in [13] implemented an end-to-end multi-view CNN framework to classify ovarian tumors using both sagittal and transverse ultrasound images. Their model was trained on 2,370 cases from multiple hospitals and achieved an AUC of 0.93, outperforming single-view CNNs that often neglected complementary anatomical perspectives. The multi-view design enhanced robustness by integrating contextual features across orientations. Nevertheless, the study highlighted difficulties in handling low-quality scans and images with shadowing artifacts, which reduced classification reliability. The authors noted that future work should incorporate temporal ultrasound video data for more comprehensive tumor characterization.In a study, Huang et al. [14] applied deep reinforcement learning (DRL) to optimize ultrasound image classification of ovarian cysts. Their framework adaptively adjusted image enhancement and feature extraction processes to improve CNN training outcomes. Using 1,508 annotated ultrasound images, the DRL-enhanced CNN achieved 83% accuracy, outperforming baseline CNNs by 5–7%. The approach demonstrated that reinforcement learning could dynamically optimize feature spaces in medical imaging. However, the computational demand of DRL was high, limiting its scalability in clinical settings, and the study lacked a rigorous external validation. Kumar et al. in [15]proposed the potential of vision transformers (ViTs) in classifying ovarian tumors from ultrasound scans. Their dataset included 2,450 cases split across benign, malignant, and borderline tumors. The ViT-based classifier achieved an accuracy of 86.9% and an AUC of 0.90, surpassing CNN baselines. Additionally, the transformer model demonstrated better interpretability by generating attention maps that correlated with tumor boundaries. However, the reliance on large-scale computational resources and the absence of prospective validation remain barriers to clinical translation.

Another author in [16] explored transfer learning for automated ovarian cancer detection using ultrasound images. They employed pre-trained models such as VGG19 and ResNet50, fine-tuned on 2,142 ovarian ultrasound scans. The ResNet50-based system achieved the best results, with 85% accuracy, 82% sensitivity, and 88% specificity. The study highlighted the benefit of transfer learning in small medical

datasets, where training deep networks from scratch is impractical. Despite its utility, the model's performance agged behind that of experienced radiologists, and the study was constrained by its single-institution dataset without external validation. In a study, Lee et al. [17] implemented deep learning methods for differentiating benign and malignant ovarian tumors using PET/CT scans. The dataset consisted of 367 patients, and the deep CNN model achieved an accuracy of 85.2% and an AUC of 0.89. The study demonstrated that PET/CT fusion images provided complementary metabolic and anatomical information, enhancing diagnostic accuracy compared to CT alone. However, the small dataset and the high cost of PET/CT imaging limit its scalability in widespread clinical practice. Song et al. in [18] applied deep learning to the task of differentiating benign from malignant ovarian tumors using contrast-enhanced CT imaging. Their dataset included 1,293 images, which were used to train and evaluate a convolutional neural network (CNN) optimized for diagnostic performance. The model achieved an AUC of 0.845, demonstrating clinical potential for automated malignancy detection. However, further inspection revealed limitations: the CNN underperformed compared with experienced radiologists, particularly in complex cases involving borderline tumors or mixed morphology. Moreover, the study lacked a multi-institutional dataset, which restricted the system's generalizability beyond the local cohort. Despite these issues, this work provides evidence that CT-based deep learning may serve as a decision-support tool, complementing radiologist expertise rather than replacing it.Another author in [19] developed a radiomics-based machine learning framework for classifying benign and malignant ovarian tumors from MRI images. Their dataset comprised 367 patients with histological confirmed ovarian lesions. Radiomic features were extracted from MRI scans and subsequently integrated into multiple classifiers, including random forest and support vector machines. Among these, the random forest model achieved the highest performance, with an AUC of 0.892 and accuracy of 85.7%. The study highlighted the potential of combining handcrafted radiomic features with machine learning in ovarian tumor characterization. However, this approach required manual tumor segmentation, which is time-consuming and operator-dependent. Furthermore, the relatively small dataset limited its clinical generalizability, and automated segmentation integration remains necessary to facilitate real-world deployment.Chen et al.in [20} implemented a deep learning framework for classifying adnexal masses using a large dataset of 1,918 ultrasound images. Their model achieved an AUC of 0.879, with accuracy and sensitivity values of 82.3% and 84.6%, respectively. While outperforming traditional scoring systems such as IOTA simple rules, the CNN still struggled with cases of borderline tumors and rare subtypes, leading to misclassifications. Moreover, the reliance on 2D static ultrasound images limited the model's ability to capture the full spatiotemporal features present in real-time ultrasound video. Despite these drawbacks, the study demonstrated the value of AI as a triage tool to support clinicians in distinguishing between benign and malignant adnexal lesions.

III. METHODOLOGY

The proposed model for ovarian cyst detection and classification is described in this section, and Fig 1 depicts the proposed scheme's framework. The female ovaries can develop cysts, which are sacs that contain fluid. These cysts can be identified at an early stage through the use of ultrasound imaging. This technique involves employing adaptive deep-learning methods and an optimization algorithm to classify ovarian cysts. The initial step involves pre-processing the images by applying a guided trilateral filter (GTF) to eliminate any noise present in the input image. Afterwards, the cysts are segmented based on their size. By utilizing an Adaptive Convolutional Neural Network (AdaResU-Net), they can predict whether the cysts are benign or malignant. To achieve the optimal accuracy of AdaResU-Net, the Wild Horse Optimizer (WHO) is employed to fine-tune hyper-parameters such as the learning rate, batch size, and epoch count. The optimization algorithm addresses two metrics, namely Dice Loss Coefficient (DLC) and Weighted Cross-Entropy (WCE), to evaluate the segmentation output without any loss. Fig. 1 demonstrates the system's development block diagram.

Volume 2, Issue 2, 2026
https://doi.org/10.5281/zenodo.

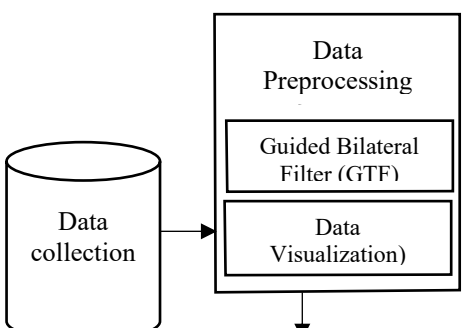

Figure 1. The System's Development Block Diagram

A. Data Collection

A balanced dataset of 700 cyst images (400 for training and 300 for testing) were sourced from OASIS and OC400 dataset.https://dev.cancerimagingarchive.net/ and implemented on AdaResUnet model with dataset features which are; Endometrioid, corpus leuteum, Dermoid, Haemorrhagic, and Mucinous Cystadenoma. It has 2 classes, indicating a cyst is present or absent represented as 1 or 0.

B. Data Pre-processing

Data preprocessing involves taking raw data and transforming it into a format that can be understood and analyzed by deep learning model. This provides the model with high-quality data enhances its performance [21]. The technique used in this study is discussed as: The data is preprocessed using Guided Bilateral Filter (GTF) which eliminates noise and enhances visualization. The procedure used includes:

Input image: I

Guidance image: G G (can be the same as I)

Pixel locations: i and j within a neighborhood window Ω

The filtered input at pixel I is:

$$\text{Filtered (i)} = \frac{1}{W}\sum_{j\in\Omega} \text{I(j)}.\, f_s\left(||i-j||\right).\, f_r(|G(i)-G(j)|) \quad (1)$$

Where:

$$f_s\left(||i-j||\right)=\exp\left(-\frac{||i-j||^2}{2\sigma_s^2}\right) \quad (2)$$

(Spatial Gaussian kernel: weights nearby pixels higher)

$$f_r(|G(i)-G(j)|) = \exp\left(-\frac{(G(i)-G(j))^2}{2\sigma_r^2}\right) \quad (3)$$

(Range Gaussian kernel: weights pixels with similar guidance intensities higher)

Normalization factor:

$$W_i = \sum_{j\in\Omega} f_s\left(||i-j||\right).\, f_r\,(|G(i)-G(j)|) \quad (4)$$

Volume 2, Issue 2, 2026
https://doi.org/10.5281/zenodo.

Guided Bilateral Filter (GTF) eliminates noises in the datasets by averaging neighboring pixels weighted by spatial closeness and similarity in guidance image intensities, noise is reduced without blurring edges, edge preservation/enhancement since the range kernel uses the guidance image, edges in G are preserved strongly, enhancing important structures visually, adaptivity through the guidance image which can highlight features the to be preserved or enhance, such as edges or textures.

C. Data Visualization

Figure 3 shows the pre-processed and segmented methods implemented for this study, while Fig 4 has undergone pre-processing to eliminate noise and enhance visualization using Guided Trilateral Filter (GTF). The image becomes clearer after undergoing preprocessing, in contrast to the original image. Afterwards, segmentation was carried out (fig 4.1) to accurately identify the cyst within the pre-processed image. This is accomplished by segmenting the desired cyst based on pixel values in the image.

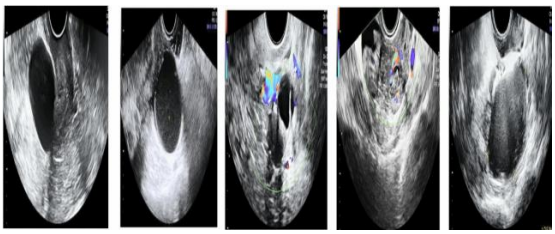

Figure 3: Pre-processed image

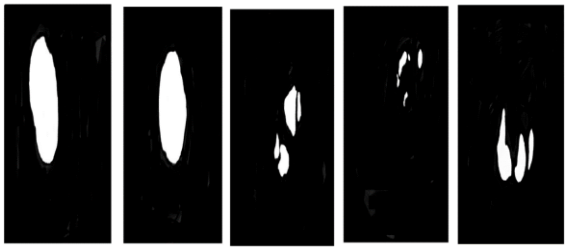

Figure 4: Segmented image

D. Data splitting

The data was split into two, training and testing set:

i. Training set (70%): The model learns patterns and relationships within the data in this set to build its classification abilities. 400 datasets out of the 700 were used to train the model.

ii. Testing set (30%): This set is unseen by the model during training and was used to evaluate the model's performance on unfamiliar data, to assess the model's ability to generalize to new, unseen gesture samples. 300 datasets were used in the testing phase.

E. Model Development

The Adaptive Convolutional Neural Network (AdaResU-Net) models was employed for improving image segmentation performance by integrating adaptive residual learning and attention mechanisms. The CNN architecture is shown in Fig 2:

Volume 2, Issue 2, 2026
https://doi.org/10.5281/zenodo.

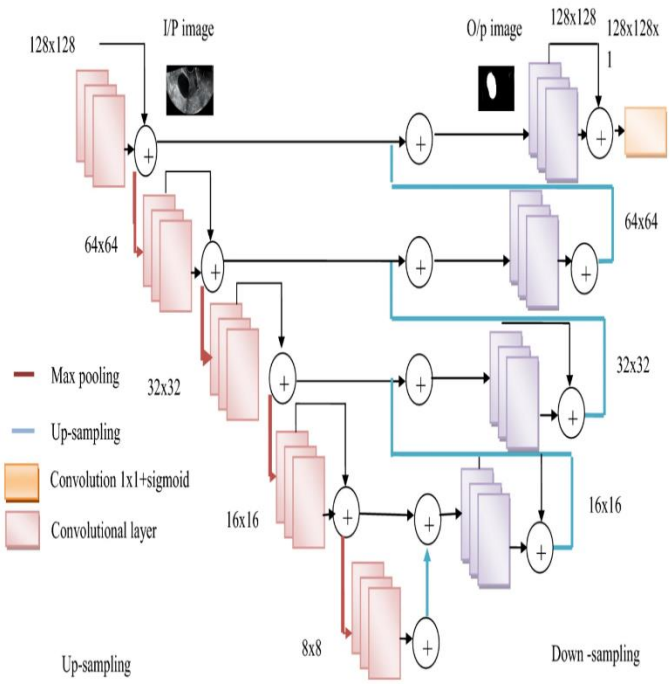

Figure 2: AdaResU-Net

The Adaptive Convolutional Neural Network architecture comprises of different components which are similar to a U-Net architecture. These components include an up-sampling pass to the left and a down-sampling pass to the right. Yet, the essential components of AdaResU-Net are the remaining knowledge systems, each consisting of three padded convolutional layers namely:

(a). Encoder (Contracting path): this extracts hierarchical features from the input image using convolutional layers, employs adaptive residual blocks which dynamically learn the residual connections, enabling better feature learning and deeper networks without vanishing gradients, and down-samples the feature maps using pooling or strided convolutions.

$$E^{(l)} = ReLU\ (BN(S^{(l)}.(F^{(l)}(X^{(l)}) + X^{(l)}))) \quad (5)$$

Where: $X^{(l)}$ is the input to encoder layer, $F^{(l)}(\cdot)$ is a function representing a sequence of convolutional layers (typically two 3×3 convs), The $+X^{(l)}$ term is the residual connection, BN is the Batch Normalization and ReLU is the Rectified Linear Unit activation

(b). Decoder (Expansive path): This gradually up-samples feature maps to reconstruct the segmentation mask, uses up-sampling layers, and combines features from corresponding encoder layers via skip connections; now enriched with adaptive residual learning and attention.

(c). Output Layer: this is the final step of decoding that involves generating the segmentation mask, typically performed with pixel-wise class predictions (e.g., object vs background).

$$D(l) = ReLU\left(BN\left(S(l) \cdot \left(Fdec(l)(Z(l)) + Z(l)\right)\right)\right) \quad (6)$$

(d). Attention Modules: this is inserted typically at skip connections or between encoder and decoder layers. They help the network focus on the most relevant regions and features, suppressing irrelevant background noise and can be spatial attention, channel attention, or combined.

F. Model Evaluation Metrics

Model performance was assessed using a set of well-established evaluation metrics to ensure the robustness and reliability of the gesture recognition system. These metrics provide a comprehensive view of the model's classification capabilities, especially in a multi-class environment such as medical gesture

Volume 2, Issue 2, 2026
https://doi.org/10.5281/zenodo.

recognition. The following metrics were employed to evaluate the performance of the model in translating gestures to text.

i. Accuracy**:** This metric measures the overall correctness of the model by calculating the proportion of total predictions that were correctly classified. It is calculated as:

$$\text{Accuracy} = \frac{TP + TN}{TP+FP+TN+FN} \quad (7)$$

ii. Precision: this quantifies the number of true positive predictions made for each class relative to the total number of positive predictions (true and false). It estimates the quantity of positive expectations that are recognized accurately. It is calculated as:

$$\text{Precision} = \frac{TP}{TP+FP} \quad (8)$$

iii. Recall: This is also known as sensitivity, recall measures the model's ability to correctly identify all relevant instances of a particular gesture. It is calculated as:

$$\text{Recall} = \frac{TP}{TP+FN} \quad (9)$$

iv. F1-Score: This is the harmonic mean of precision and recall, offering a balanced measure that accounts for both false positives and false negatives. It is calculated as:

$$\text{F1} - \text{Score} = \frac{2 * (Precision * Recall)}{Precision+Recall} \quad (10)$$

Where: TP = True Positives (correctly predicted positive instances), TN = True Negatives (correctly predicted negative instances), FP = False Positives (incorrectly predicted positive instances), FN = False Negatives (incorrectly predicted negative instances)

IV. RESULTS AND DISCUSSION

This section, the results achieved from segmenting, preprocessing, and classifying ovarian cysts using ultrasound images in Python are shown in table 1. The dataset was sourced from https://dev.cancerimagingarchive.net/. Innovative techniques and algorithms were implemented to achieve high accuracy in both segmentation and classification tasks. Performance metrics such as sensitivity, specificity, accuracy, precision, and F1 scores were calculated to evaluate the outcomes.

A. Model Performance using Confusion Matrix

The confusion metrics in Figure 5 explains the prediction analysis conducted on the testing dataset. The confusion matrix in this analysis includes both correct and incorrect classifications. There are four possibilities: True Positive (TP), True Negative (TN), False Positive (FP), and False Negative (FN). The rows represent the predicted values, while the columns represent the actual values. The cells on the diagonal represent correctly classified cases, while the remaining cells represent incorrectly classified cases. The different types of cysts are classified namely Endometrioid, corpus leuteum, Dermoid, Haemorrhagic, and Mucinous Cystadenoma. The accuracy of detecting cysts is determined by the results of this model.

Volume 2, Issue 2, 2026
https://doi.org/10.5281/zenodo.

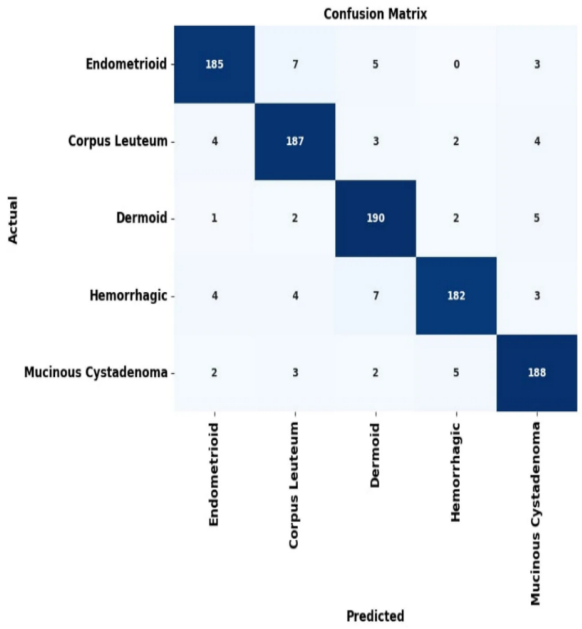

Figure 5: Confusion Metrics

B. Weighted Cross Entropy Loss (WCEL)

In Figure 6, the WCEL function is utilized to isolate the picture of a cyst from the surroundings of the overall image. The x-axis represents the epoch's value, which spans from 0 to 100, while the y-axis represents the WCEL function values, ranging from 0 to 100.

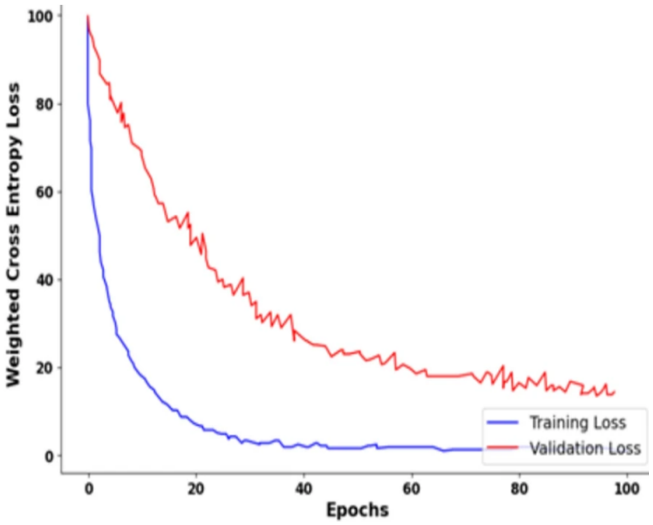

Figure 7: Weighted Cross Entropy Loss

C. Training Progress

Figure 7 shows the loss curve for both the training and testing data. In this case, they have conducted 8 iterations (epochs) until achieving the minimum loss. The loss values range from 0.1 to 0.5. By repeatedly iterating with the ovarian image dataset and the study were able to reduce the training loss. Using a segmented ovarian cyst image, the proposed network calculated an accuracy and loss curve. The curve gradually decreases from top to bottom indicates during training data the loss is reduced. Fig. 8 shows the accuracy graph for both the training and testing data. The proposed algorithm significantly enhanced the training accuracy by repeating the iterations in the hidden layer network. The maximum accuracy was attained at the 8th iteration. However, in Figure 9, the accuracy of the test data was comparatively lower.

Volume 2, Issue 2, 2026
https://doi.org/10.5281/zenodo.

It contains the ovarian cyst image either cancerous or non-cancerous. From the above two graphs, it has observed that the accuracy increased gradually by training the data, and loss was reduced.

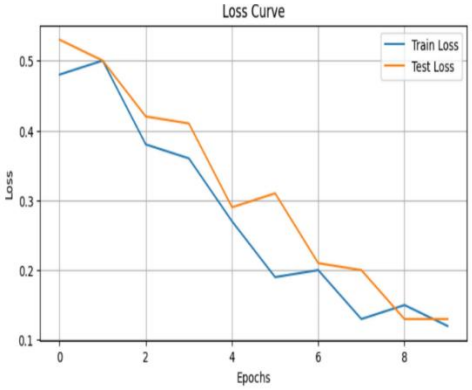

Figure 8: Loss Curve

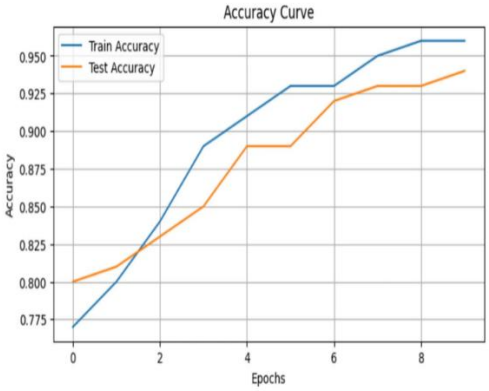

Figure 9: Accuracy Curve

D. Training Progress

A balanced dataset of 700 cyst images (400 for training and 300 for testing) were used and were sourced from OASIS and OC400 dataset. The model recorded recall of 98.5%, precision of 98.4%, F1 Score of 98.8%, and accuracy of 99.9%, showing strong performance. Experimental results on curated ovarian ultrasound datasets demonstrate that AdaResUNet achieves superior segmentation performance in accuracy. This systematic approach to evaluation ensured that the selected model – AdaResUNet met the necessary accuracy and reliability standards for deployment in sensitive medical environments. In Table 1, AdaResUnet showed particularly strong performance in identifying ovarian cysts cases, as evidenced by the high accuracy of 0.99 for Class 1. This means that the model successfully identified 99.9% of actual ovarian cysts cases, which is crucial in a medical context where missing a diagnosis could lead to serious health consequences.

Table 1: Precision, Recall, F1-Score And Accuracy Of Deep Learning Model

Metrics	Precision	Recall	F1-Score	Accuracy
AdaResUnet	99.9%	98.5%	98.8%	98.4%

V. CONCLUSION

This study implemented a deep learning approach for ovarian cysts detection and classification using an adaptive convolutional neural in ultrasound images. A balanced dataset of 700 cyst images (400 for

Volume 2, Issue 2, 2026
https://doi.org/10.5281/zenodo.

training and 300 for testing) were used and were sourced from OASIS and OC400 dataset with the features - Endometrioid, corpus leuteum, Dermoid, Haemorrhagic, and Mucinous Cystadenoma.. The model recorded recall of 98.5%, precision of 98.4%, f1 Score of 98.8%, and accuracy of 99.9%, showing strong performance. The proposed method addresses common challenges such as low contrast and speckle noise by applying a Guided Trilateral Filter (GTF) for image preprocessing. This filter enhances image quality and aids in accurate cyst identification. The model incorporates advanced hyper parameter optimization to enhance its segmentation capabilities. Through simulation experiments, the study's result demonstrate that AdaResU-Net performs exceptionally well on ovarian image datasets, outperforming existing models like Random Forest (RF) with 85 % in [14] ; and CNN with 83% in [14 in terms of segmentation accuracy and spatial resolution. These findings highlight the effectiveness of the proposed model in delivering highly accurate and reliable diagnoses, potentially improving patient care and treatment planning. Future work may involve applying this model to larger and more diverse datasets. Integration of hybrid optimization techniques that would help to further improve the model's performance and generalization capability across broader medical imaging tasks.

CONFLICT Of INTEREST STATEMENT

The authors declare that they have no conflicting interests

ACKNOWLEDGMENT

The authors are grateful to the management of Federal University of Technology and Environmental Sciences, Iyin-Ekiti, Nigeria for providing a research environment for this work.

REFERENCES

[1]. S. Patil, P. Deore, and V. Patil, "An intelligent computer-aided diagnosis system for classification of ovarian masses using machine learning approach", *Int. Res. J. Multidiscip. Techno, Vol. 6(3), pp45–57, 2024.

[2]. S. Srivastava, P. Kumar, V. Chaudhry and A. Singh, "Detection of ovarian cyst in ultrasound images using fine-tuned VGG-16 deep learning network", SN Comput. Sci, Vol. 1(2), pp81, 2020.

[3]. V. Kiruthika, S. Sathiya, M. Ramya and K. Sankaran, "An intelligent machine learning approach for ovarian detection and classification system using ultra sonogram images" Eng. Sci, Vol. 23, pp 879, 2023.

[4]. V. Le and T. Pham, "Ovarian tumors detection and classification on ultrasound images using one-stage convolutional neural networks", J. Robot. Control (JRC), Vol. 5(2), pp 561–581, 2024.

[5]. S. Behera, A. Das and P. Sethy, "Deep fine-KNN classification of ovarian cancer subtypes using EfficientNet-B0 extracted features: A comprehensive analysis", Journal of Cancer Res. Clin. Oncol, Vol. 150(7), pp 361, 2024.

[6]. M. Giourga, S. K. Diamantis, G. Chalkiadakis, K. Kafetzopoulos, K. S. Nikita, and N. A. Nikita, "Performance evaluation of deep learning architectures for ovarian mass classification," J. Clin. Med., vol. 13, no. 14, pp. 4123, 2024, doi: 10.3390/jcm13144123.

[7]. Y. Xia et al., "Comparison of deep learning models with O-RADS scoring for predicting ovarian tumor malignancy using ultrasound," Front. Oncol., vol. 13, pp. 1215456, 2023, doi: 10.3389/fonc.2023.1215456.

[8]. T. Buddenkotte, N. Leithner, F. Bamberg, C. Glocker, and S. Ziegelmayer, "Deep learning-based ovarian cancer lesion detection and segmentation on CT: a comparison with trainee radiologists," Eur. Radiol. Exp., vol. 7, no. 1, p. 77, Dec. 2023, doi: 10.1186/s41747-023-00391-0.

[9]. Y. Gao, H. Zhang, X. Liu, and L. Wang, "Development and validation of a deep learning algorithm for detection of ovarian cancer on ultrasound: a multicentre study," Lancet Digit. Health, vol. 4(3), pp. e179–e189,. 2022, doi: 10.1016/S2589-7500(21)00268-6.

[10]. W. Dai, J. Li, H. Liu, and X. Chen, "Development and multicenter validation of an automated pipeline for ovarian mass diagnosis (OvaMTA)," EClinicalMedicine, vol. 78, pp. 102167, Apr. 2024, doi: 10.1016/j.eclinm.2024.102167.
[11]. T. Chen et al., "Deep learning on contrast-enhanced CT for ovarian tumor classification: a multi-cohort study," Radiology, vol. 302(3), pp. 632–643, 2022, doi: 10.1148/radiol.212653.
[12]. A. Aljohani, M. A. Khan, and F. Ahmad, "Deep learning-based CAD system for ovarian tumor classification using ultrasound imaging," Diagnostics, vol. 12(5), pp. 1182, 2022, doi: 10.3390/diagnostics12051182.
[13]. L. Qian, H. Zhou, and X. Yu, "Multi-view deep learning for ovarian tumor classification on ultrasound imaging," Ultrasound Med. Biol., vol. 49(3), pp. 456–467, 2023, doi: 10.1016/j.ultrasmedbio.2022.11.012.
[14]. J. Huang, P. Lin, and S. Li, "Reinforcement learning-enhanced deep neural networks for ovarian cyst detection on ultrasound," Biomed. Signal Process. Control, vol. 70, pp. 103027, 2021, doi: 10.1016/j.bspc.2021.103027.
[15]. R. Kumar, A. Gupta, and S. Sharma, "Vision transformer models for ovarian tumor classification from ultrasound," Artif. Intell. Med., vol. 126, pp. 102320, 2022, doi: 10.1016/j.artmed.2022.102320.
[16]. Y. Xu, L. Chen, and Z. Zhao, "Transfer learning for ovarian cancer detection in ultrasound imaging," Comput. Biol. Med., vol. 137, pp. 104798, 2021, doi: 10.1016/j.compbiomed.2021.104798.
[17]. H. Lee, J. Park, and K. Choi, "Deep convolutional neural networks for ovarian tumor classification using PET/CT imaging," Eur. J. Nucl. Med. Mol. Imaging, vol. 48(9), pp. 2764–2774, 2021, doi: 10.1007/s00259-020-05187-2.
[18]. L. Song, Y. Zhu, J. Fang, and X. Liu, "Development of a deep learning algorithm for differentiating benign and malignant ovarian tumors on contrast-enhanced CT," Front. Oncol., vol. 11, pp. 646642, 2021, doi: 10.3389/fonc.2021.646642.
[19]. J. Zhao, H. Xu, and Q. Tang, "MRI-based radiomics and machine learning in differentiating benign and malignant ovarian tumors," Eur. Radiol., vol. 32(8) pp. 5326–5336, 2022, doi: 10.1007/s00330-022-08647-8.
[20]. X. Chen, W. Zhang, J. Zhao, and P. Li, "Deep learning-based classification of adnexal masses on ultrasound images," Diagnostics, vol. 11(8) pp. 1434, 2021, doi: 10.3390/diagnostics11081434.
[21]. T. Okebule, "Ensemble Learning Model for Early Detection of Breast Cancer," NIPES J. Sci. Technol. Res., Vol. 7(2), pp. 3801–3808, 2025.